

Study on Propagation Characteristics of 5G Millimeter-Wave Wireless Communication Systems for Dense Urban Environments

A Thesis Submitted to the Department of Computer Science and Communications Engineering,
the Graduate School of Fundamental Science and Engineering of Waseda University
in Partial Fulfillment of the Requirements for the Degree of Master of Engineering

Submission Date: February 1st, 2019

By

Ahmad Shahpoor Seraj
(5117FG12-7)

Advisor: Prof. Takuro Sato

Research guidance: Research on Ubiquitous Communication System

Acknowledgement

Foremost, all praise be to Allah, the Creator of this phenomenal universe Who bestowed humankind the wisdom to think and talk, and to exploit His myriad blessings all over the world for the benefit of humanity through knowledge.

Firstly, I wish to thank my advisor Prof. Takuro Sato for his patient guidance, constant support and insightful recommendations during my studies. Indeed, it has been a blessing being a member of Sato Lab, where my professional and personal life was enriched through his inspiring comments, kind advices, and continued encouragements. I also wish to express my gratitude to the faculty at Waseda University and the management team for their continued support.

I would like to sincerely thank my parents, for their unconditional love, affection and kindness. Their constant assurance and support have been a source of strength and encouragement. I am indebted to them for the great sacrifices they made to keep me moving forward. I am thankful for my parents-in-law for their affection and continued kindness. I also wish to thankfully appreciate the affection, support and kindness of my sisters and brothers. May Allah keep all of them always blessed.

I would like to thank my advisor at Kabul University, Prof. Mohammad Shafi Sharifi for his constant support, kind advices, and continued encouragements as well.

Also, I would like to greatly thank Japan International Cooperation Agency (JICA) and PEACE Project team for providing me this opportunity to explore new horizons in my professional life. Indeed, the generous scholarship from JICA made this journey and study possible. Last, but by no means least, I offer my sincerest gratitude to my wife, Zohra Ghaior, and my love for my little daughter Darya Jan, for all the joy and happiness they have brought to my life and for all their patience, support, and encouragement. You are amazing!

Abstract

Numerous recent studies on future mobile communications have considered and proposed millimeter wave (mmWave) communication as a key enabling technology for the realization of massive connectivity in the 5G and beyond era. However, the propagating signals at mmWave suffers from high propagation loss and sensitivity to blockage, resulting for high outage probability and low signal to noise ratio (SNR). This thesis discusses the propagation characteristics of mmWave and presents results of simulations on 4 GHz, 28 GHz and 73 GHz for 5G Cellular in the dense urban environments. The simulations are performed with the MATLAB-based NYUSIM simulator to evaluate the performance of mmWave channel characteristics. The results of simulations are compared with previously conducted field measurements of other studies. Our research presents large-scale characteristics of mmWave such as path loss, delay spread and power delay profile for both line-of-sight (LOS) and non-line-of-sight (NLOS) cases. The work also compares directional and omnidirectional propagation in a relatively smaller microcell with 5 times larger cell to observe the performance differences and characteristics of different mmWave frequencies with the increase in the Tx-Rx distance. Our work shows that mmWave communications is feasible for all 5G deployments within the range of microcell of up to 100 m for frequencies such as 73 GHz and up to 500 m for lower frequencies such as 4 GHz to be utilized in the dense urban areas.

***Index terms*—Millimeter wave cellular; Fifth Generation (5G); propagation characteristics; dense urban networks; channel characteristics; 4 GHz; 28 GHz; 73 GHz**

Table of Contents

Acknowledgement	i
Abstract.....	ii
Table of Contents	iii
Abbreviations	v
List of Figures.....	vii
List of Tables.....	viii
Chapter 1 Introduction.....	1
1.1 Background.....	1
1.2 Objectives and Contributions of Thesis.....	4
1.3 Organization of Thesis.....	4
Chapter 2 Literature Review	6
2.1 Development of Wireless Communications	6
2.2 An overview of 5G Cellular Systems	8
2.3 Dense Urban Deployments	11
2.4 Millimeter Wave as a Key Enabling Technology.....	12
Chapter 3 Millimeter Wave Propagation.....	14
3.1 Introduction.....	14
3.2 Millimeter Wave Spectrum	15
3.3 Propagation Characteristics of MmWave at 5G Bands	18
3.3.1 Atmospheric losses.....	18
3.3.2 Rain attenuation	20
3.3.3 Material Penetration.....	20
3.4 Summary.....	21
Chapter 4 Millimeter Wave Channel Modeling and System Design Consideration.....	22
4.1 Introduction.....	22
4.2 The Millimeter Wave Channel Model	22
4.3 Modelling Efforts in Millimeter Wave	23
4.4 Millimeter Wave Channel Modeling Challenges	25
4.5 System Design Consideration	26
4.5.1 General Structure of mmWave Channel.....	26
4.5.2 LOS Probability Model.....	27

4.5.3	Large-Scale Path Loss Models.....	28
4.6	Considered Model for Urban Dense Environments	31
Chapter 5	Performance Evaluation and Discussion	32
5.1	Simulation Setup	32
5.2	Simulation Results.....	34
5.2.1	Dense urban microcell (UMi) scenario	34
5.2.2	Dense urban macro (UMa) scenario	41
Chapter 6	Conclusion and Future Work	44
6.1	Conclusion	44
6.2	Future Work	45
	Research Achievements.....	46
	References.....	47

Abbreviations

5G	Fifth Generation
BER	Bit Error Rate
BF	Beamforming
CI	Close in
D2D	Device-to-Device
ETSI	European Telecommunications Standards Institute
FSL	Free-Space Loss
HetNet	Heterogeneous Network
LOS	Line-of-Sight
METIS	Mobile and wireless communications Enablers for the Twenty-twenty Information Society
MIMO	Multiple-Input Multiple-Output
mmWave	Millimeter Wave
MPC	Multipath component
NLOS	Non-Line-of-Sight
O2i	Outdoor-to-indoor
OFDM	Orthogonal Frequency Division Multiplexing
PDP	Power delay Profile
PL	Path Loss
PLE	Path Loss Exponent
PTP	Point-to-Point
QoS	Quality of Service
RX	Receiver
SCM	Special Channel Model
SNR	Signal-to-Noise-Ratio

TX	Transmitter
UMa	Urban Macro
UMi	Urban Micro
V2V	Vehicular-to-Vehicular
WLAN	Wireless Local Area Network
ISD	Inter site Distance
EHF	Extremely High Frequency
SHF	Super High Frequency
TH	Tera Hertz
eMBB	enhanced Mobile Broadband
MMS	Multimedia Messaging Service

List of Figures

Figure 2.1 Development of wireless communications and evolution of cellular networks [10]	8
Figure 2.2 Usage scenarios for IMT 2020 and beyond [12], [32]	9
Figure 3.1 Millimeter wave spectrum, along with oxygen and water vapor absorption bands [7]	16
Figure 3.2 Specific attenuation of <i>O2</i> , <i>H2O</i> and rain at sea level [39]	19
Figure 5.1. Omnidirectional and directional path loss values generated with 500 simulation runs for the 28 GHz UMi, (a) LOS and (b) NLOS scenarios. n denotes the path loss exponent (PLE), σ is the shadow fading standard deviation, "omni" represents omnidirectional, "dir" denotes directional, "dir-best" means the direction with the strongest received power, "Ant." denotes antenna, "AZ" and "EL" stand for azimuth and elevation, respectively.....	36
Figure 5.2 Omnidirectional PDP and Directional Power Delay Profiles with strongest power at 28 GHz at 200.8 m TX-RX separation in UMi LOS case. "Ant." denotes antenna.....	38
Figure 5.3 Omnidirectional and directional path loss values generated with 500 simulation runs for the 73 GHz UMi, (a) LOS and (b) NLOS scenarios.....	39
Figure 5.4 Omnidirectional PDP and Directional Power Delay Profiles with strongest power at 73 GHz at 101.9 m UMi LOS case. "Ant." denotes antenna.....	40
Figure 5.5 Omnidirectional and directional path loss values generated with 500 simulation runs for the 4 GHz UMa, (a) LOS and (b) NLOS scenarios.....	42
Figure 5.6 Omnidirectional PDP and Directional Power Delay Profiles with strongest power at 4 GHz at 499.6 m UMa NLOS case. "Ant." denotes antenna.....	43

List of Tables

Table 2.1	Minimum requirements of IMT 2020 and beyond [32]	10
Table 3.1	Millimeter wav frequency bands designation for sub-100 GHz [41]	16
Table 3.2	Considered mmWave bands for 5G by different organizations [40]	17
Table 3.3	Penetration losses of different materials in dB/cm based on the measurements by [18]	21
Table 4.1	mmWave channel modeling by different organizations and efforts [9]...	24
Table 4.2	LOS Probability models of 5GCM in the UMi and UMa Scenario [48]...	27
Table 4.3	Omnidirectional path loss models in the UMi scenario [48]	30
Table 4.4	Omnidirectional path loss models in the UMa scenario [48]	31
Table 5.1	Channel parameters and antenna properties for UMi and UMa scenarios	33

Chapter 1

Introduction

1.1 Background

Wireless communication has witnessed very rapid growth in the past two decades and has become pervasive in our world. The most recent development in this field is application of millimeter wave (mmWave) band in the existing and emerging wireless systems deployments [1]. Recent studies show that the exponential growth in demand for data traffic will continue in the next decade, in which for example, global traffic annually will reach 4.8 Zettabytes (ZB) or 396 Exabytes (EB) per month by the end of 2022, which is more than three times of 1.5 ZB per year and 122 EB per month, recorded for 2017 [2].

Cisco forecasts in [2], that Wi-Fi and mobile devices will account for 71 percent of worldwide traffic by 2022, which was only 52 percent in 2017, meanwhile, mobile data traffic will increase sevenfold from 2017 to 2022 at a 46 percent growth rate annually reaching 77.5 EB per month which will account for 20 percent for all IP traffic data. Comparing the estimated data traffic between 2022 in [2] and the recorded data traffic in 2012 in [3], which shows more than nine fold increase, from 43.6 EB per month to 396 EB per month, it seems that it was a real alert that the challenge of capacity demand

sparked the efforts of both academia [4], [5], [6] and industry [7], [8] for finding new methods to overcoming it. Conventionally, reducing the cell size and proposing the advanced techniques of signal processing are used to enhance the system capacity, yet another powerful technique is to allocate large frequency spectrum such as the enormous amount of spectrum in mmWave bands for the usage in cellular networks [9].

Numerous recent studies on future mobile communications have considered and proposed mmWave communication as a key enabling technology for the realization of the Internet of Things (IoT) in the 5G and beyond era [1], [4], [10], [11]. The 5G network is expected to support extremely large amounts of wireless traffic data and realize massive connectivity, while achieving better quality of service, energy-efficiency and reliability, and with lower communication delay [1], [12], [13], [14]. The enormous amount of spectrum in the mmWave bands which is unparalleled compared to sub-6 GHz bands, along with introducing small cells and advanced signal processing techniques will provide unprecedented radio resource capacity for 5G and beyond wireless networks and will meet the capacity demand for traffic in the years to come [1], [9], [15], [16].

There are fundamental differences between existing wireless communication networks and future mmWave cellular communication, in which some of them are directivity, propagation loss, and sensitivity to blockage [1], [9], [10]. These differences pose several challenges in utilizing the full potentials of mmWave communications. To ensure an interference-free and reliable communication network in mmWave bands, efficient antennas with high directionality and massive antenna elements (AEs) are required to meet the massive connectivity especially in the dense urban environments. [4], [14]. To facilitate studying the 5G requirements and to provide technical design guidance, several deployment scenarios, have been proposed for 5G in literature [12], [17]. The need for availability of a heterogenous network such as 5G for the dense urban environments seems urgent. The growing number of connected devices, with high

traffic loads, outdoor, and outdoor to indoor coverage are the characteristics of this environment [12]. The deployment of 5G mmWave network in this environment is limited by several factors as well. The availability of buildings usually composed of concrete, bricks, glass, wood, etc., with the harsh characteristics of mmWave for penetration to these materials, and high atmospheric effects on mmWave compared to sub-6 GHz bands, causes high attenuation for the propagating signal and poor signal to noise ratio (SNR) [18].

As [9] reported, in order to study mmWave use cases for 5G, most of the measurement campaign as in [4], [18], [19] concentrated on dense urban environments. Based on the mentioned measurements, several channel models have been proposed. Since the considered mmWave bands for 5G deployments is very huge and is not financially and technically feasible to do measurement for the whole bandwidth, researchers are studying mmWave 5G conducting simulations to evaluate the propagation characteristics of mmWave for the 5G network.

The purpose of this research is to focus on finding innovative solutions addressing the challenges of severe attenuation, antenna design and limiting propagation characteristics for 5G mmWave-enabled systems and applications. The focus of this work is on emerging antenna arrays for the usage in the portable mmWave devices and systems and not on fixed antennas of conventional microwave or fixed mmWave wireless systems. Therefore, the aim is to study the large-scale fading parameters of mmWave-enabled 5G systems propagations with a massive MIMO antenna in dense urban areas through comparing simulations with various already measured data such as in [18] and [20]. The focus of this research is on the propagation characteristics in the 4 GHz, 28 GHz and 73 GHz bands as candidate and trialed bands for 5G deployment [20], [30].

1.2 Objectives and Contributions of Thesis

As the usage of massive multiple input and multiple output (MIMO) and millimeter wave communication for the dense 5G cellular network will be a reality soon, studying and investigating the related challenges, and evaluation of the performance of the 5G network is among the main objectives of this thesis, which in turns, will contribute to the ongoing research on as the following.

- To effectively and efficiently use the mmWave spectrum in the heterogenous 5G deployments for the dense urban environments, we propose a heterogenous dense cellular network architecture with a maximum radius cell of 100 m for 73 GHz, 200 m for 28 GHz and 500 m for 4 Ghz.
- To study the large-scale parameters such as path loss and shadow factor of propagation at mmWave bands and to verify the performance of the 5G network, we use the software simulation.
- The other contribution is the study of 4 GHz propagation for 5G cellular network. Although 4 GHz has already been utilized in some applications, mobile communication will witness a large band in sub-6 GHz in 5G system.

1.3 Organization of Thesis

The rest of this thesis is structured as follows:

- Chapter 2 reviews the literature on the evolution of the emerging cellular networks. The development of communication systems in recent years is discussed which will be followed by overviewing of 5G cellular networks. Then, the dense urban environment is introduced and its requirements in the

5G systems. The importance of millimeter wave as an enabling technology is briefed as well.

- Chapter 3 provides a review on propagations at mmWave with the focus on the propagation characteristics on 5G bands. The millimeter wave spectrum is discussed and the propagation characteristics including the atmospheric effects on mmWaves is overviewed. Free space path loss, atmospheric losses, rain attenuation, and material penetration at mmWaves are explained. The applications of mmWave are reviewed which is followed by a summary.
- In chapter 4, mmWave channel models, and accordingly system design is discussed. The mmWave channel modelling efforts and related challenges is studied and followed by introducing the system design consideration, model and scenario which will be used in this thesis.
- Chapter 5 presents our results of simulations in the 4 GHz, 28 GHz and 73 GHz bands for the 5G urban dense networks. The simulation results with consideration of UMi and UMa are discussed in details and different scenarios such as LOS and NLOS performance of the mentioned frequency bands are evaluated.
- Finally, in chapter 6, we draw our conclusion based on the findings from previous chapters and present a study direction at the end of the same chapter.

Chapter 2

Literature Review

2.1 Development of Wireless Communications

The first wireless networks, by means of smoke signals, flashing mirrors, or semaphore flags, etc., were developed long before industrial revolution. More than one hundred and twenty years ago, Guglielmo Marconi demonstrated the first radio transmission, in mid 1890s, and era of radio communication started [21], [22]. Since then, wireless communications have evolved continually, and new methods and systems were introduced. A new era of wireless communication was born in the 1960s and 1970s after the introduction of cellular concept, and advancement in radio frequency hardware [22].

Today, wireless communication is the fastest growing engineering field with its wide spread applications prevailed in all aspects of 21st century humankind life. According to T.S. Rappaport et al. in [4], since the new era and the beginning of 1980, every 10 years has witnessed a new generation of wireless communication systems with more advanced technology in terms of data rate, spectrum efficiency, coverage and applications.

Although early wireless Local Area Networks (LANs) could not compete with wired Ethernet technology, the most successful application of wireless communication has been the cellular systems [21]. The 1st generation (1G) cellular was announced at the beginning of 1980's, which was an analog system with a few kbps data rates and a lot of disadvantages. In 1993, the 2nd generation (2G) was introduced, which is a digital technology mainly used for voice communication and new capabilities such as roaming and Short Message Service (SMS) and with a bit rate of up to 64 kbps. Global System for Mobile communications (GSM) and Code Division Multiple Access (CDMA) and IS-95, were the famous technologies of 2G [10]. The data rate was improved by introducing upgrades into 2G, such as General Packet Radio Service (GPRS) and Enhanced Data Rate for GSM Evolution (EDGE) to 144 kbps and 384 kbps respectively [10].

The 3rd generation was introduced in 2000 with new technologies and features. The initial transmission rate was 2Mbps which was improved up to 30Mbps as the evolving technologies such as High-Speed Uplink/Downlink Packet Access (HSUPA/HSDPA) were added to the network [10]. The 3rd Generation Project Partnership (3GPP) introduced Long Term Evolution (LTE) technology as the descendant of previous cellular generations which is considered as 4G and was followed by LTE-Advanced with even higher bit rate. The higher bit rate compared to 2G and 3G, and new applications such as Multimedia Messaging Service (MMS), Digital Video Broadcasting (DVB) and High Definition (HD) mobile TV are among the features 4G operators offer to the subscribers [10].

As cisco estimates in [2], the exponential growth in the demand for higher data traffic, and the other challenges 4G LTE is currently facing in terms of capacity, end to end latency, massive device connectivity, quality of service and cost [12], it is assumed must be addressed by 5G, a new generation of cellular networks with new features and new technologies. Evolution of 1G to 4G is shown in the Figure 2.1 from [10]. It shows

how the generations of wireless systems develops in terms of data rate, mobility, spectral efficiency and coverage. All these features increase when a new generation evolves. It also shows changing nature of the generations from circuit switched to packet switched and from fixed to vehicular along with differentiating between licensed and unlicensed spectrums. The next section will present a detailed overview of 5G and how it will address the challenges available toward its utilization.

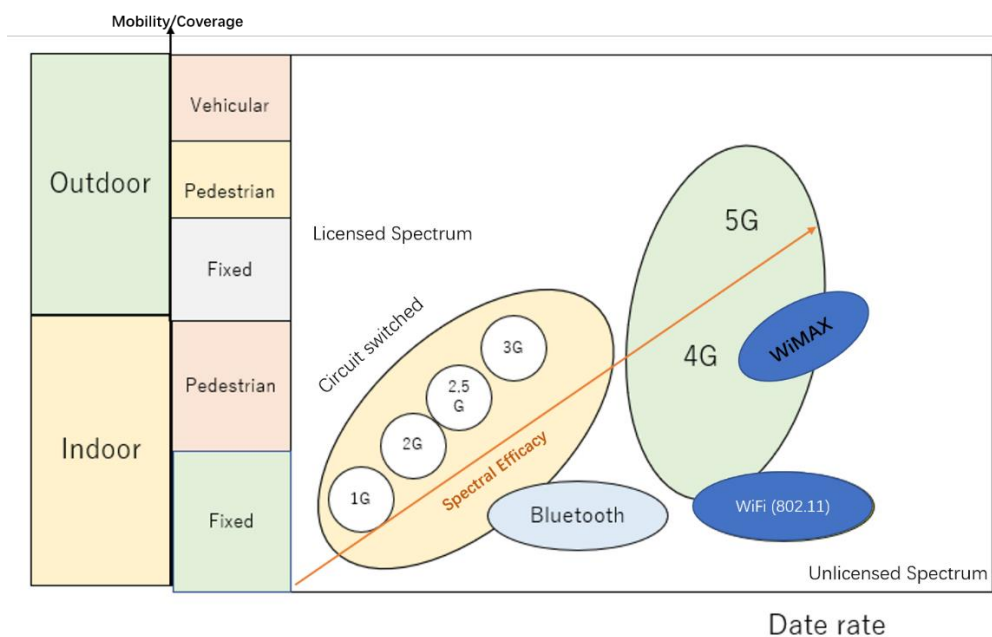


Figure 2.1.1 Development of wireless communications and evolution of cellular networks [10]

2.2 An overview of 5G Cellular Systems

With the explosive growth of mobile traffic and exponentially increase in the demand of users for new services and applications, 5G mobile systems are now being designed to fulfill the requirements of these services, in terms of data rate, latency, reliability, and with low cost and massive connectivity. The early researches on

different aspects of 5G cellular system appeared in literature in mid-2013 [23], and after of the start of working on vision Recommendation of ITU-R for IMT-2020 in 2012.

From that year on, several programs and projects initiated globally to deeply study 5G and its enabling technologies in the years to come. The academia and industry under the following major projects such as the European Union framework program for research and innovation (Horizon 2020) [24] and 5G Infrastructure Public Private Partnership (5GPPP) [25] in Europe, NYU WIRELESS research center [26] and 5G Americas [27] in the United States, IMT-2020 (5G) Promotion Group in China [28], 5G forum in Korea [29], the 5G Mobile communications promotion Forum (5GMF) [30] in Japan, have been actively promoting 5G research and development, in which in parallel 3GPP [31] and other concerned standardization bodies are finalizing the 5G NR and related standards.

The emerging applications and new services for the mobile communications in 2020 and beyond, and key capabilities and minimum requirements of IMT-2020 for the realization of envisioned usage scenarios was released in the ITU-R [32] in 2015. Some instance of enviroined usage scenarios for IMT for 2020 and beyond are depicted in Figure 2.2 [32].

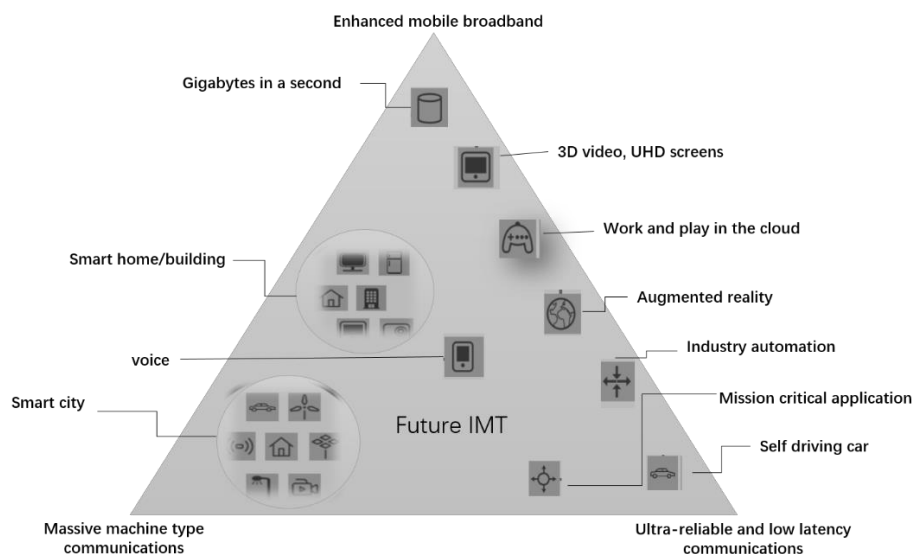


Figure 2.2 Usage scenarios for IMT 2020 and beyond [12], [32]

Figure 2.2 shows the three main use cases of enhanced Mobile Broadband (eMBB), massive machine type communications and ultra-reliable and low latency communications, for different applications and various technical requirements for IMT for 2020 and beyond.

To fulfil the requirement for the envisioned applications and usage scenarios, ITU-R introduced some new capabilities with enhancements compared to the IMT-Advanced of 2012, as shown in Table 2.1[32].

Table 2.1 Minimum requirements of IMT 2020 and beyond [32]

Main capabilities	Values
Peak data rate	20 Gbps
User experienced data rate	0.1-1 Gbps
Latency	1 ms over-the-air
Connection density	10^6 /km ²
Mobility	500 km/h
Energy efficiency	100 x IMT-advanced
Area Traffic capacity	10 Mbit/s/m ²
Spectrum efficiency	(3-5) x IMT-Advanced

According to ITU-R, the values in the figure are milestones for the research and investigation and may be revised and developed based on the new findings.

To find and examine the technologies meeting the proposed requirements, Rappaport et al. in [4], and S. Sun et al. in [33] presented the results of extensive measurements and proposed millimeter Wave for 5G cellular. Authors in [15], [34], [35] and [36] proposed beamforming (BF) and massive Multiple-Input Multiple-Output (MIMO)

with highly directional antenna arrays to mitigate the harsh propagation characteristics of mmWaves for 5G. Small cells with heterogenous systems for 5G was discussed in [11] and [39]. Along with these, network slicing for 5G was discussed in [37] and authors in [10] presented a general heterogenous architecture for 5G cellular and its emerging technologies and depicted how a heterogenous network combining of microcell, small cells, 5G Wi-Fi, D2D communication, wireless sensor networks along with massive MIMO and so on, will be used for 5G.

As authors in [12] and numerous other researchers proposed the idea of splitting indoor and outdoor setups for 5G, and because of high penetration losses that millimeter wave have [41], our focus in this work is mainly on the outdoor environments, and indoor scenarios are beyond the scope of this thesis. In the following subsections, we will briefly review how dense urban environment will attract much of 5G use cases, and how millimeter wave will be a key enabling technology for the 5G dense urban environment deployments.

2.3 Dense Urban Deployments

The densification of cellular networks for the 3G intended to improve the transmission rate, with a density of 4-5 BSs/km². For the 4G LTE-A, hotspot and femtocell BSs have been deployed with a density of 8-10 BSs/km². To satisfy the requirements of 5G and benefiting the massive MIMO and millimeter wave technologies, the density of 5G is anticipated to be 40-50 BSs/km², making it an ultra-dense cellular network [38].

Out of the 10 deployment scenarios studied by 3GPP [31], dense urban scenario is among the scenarios proposed for enhanced mobile broadband (eMBB). In this heterogeneous deployment scenario, the focus is on macro cells with micro cells in city centers and dense urban areas with high user densities. The main characteristics of this

scenario are outdoor and outdoor-to-indoor coverage with high traffic loads. In this scenario, the Inter-Site-Distance (ISD) of the macro cells is 200 m, containing 3 micro cells. The heights for macro cells and micro cells are 25 m and 10 m respectively. The carrier frequency for macro cell is 4 GHz and for micro cells includes around 30 GHz and around 70 GHz as well. The bandwidth for 4 GHz is up to 200 MHz and expands up to 1GHz for both around 30 GHz and around 70 GHz. In this scenario, 80 % of users are indoor having a speed of 3 km per hour and 20 % are in cars with a moving speed of 30 km per hour. [12], [32]. The motivating idea behind this densification in 5G networks seems to be the promising capabilities of millimeter wave which will be briefly reviewed in next section.

2.4 Millimeter Wave as a Key Enabling Technology

The rapid growth of wireless and mobile traffic and the global bandwidth shortage in sub-3 GHz bands has encouraged the exploration and use of underutilized millimeter wave spectrum to meet the requirements in 5G and beyond networks [4], [40]. The huge bandwidth of millimeter wave with much smaller antenna sizes which makes it possible to fit more antennas into a small printed circuit board, small package or on a chip, and massive MIMO, provide high data rates which are required in different 5G scenarios [1]. Many researches have investigated and showed that mmWave communication can be used in different aspects of 5G, from small cell access providing multi-gigabit transmission rate and cellular access for high capacity and coverage when densely deployed, to wireless backhaul replacing the fiber based backhails, still maintaining several Gbps data rates [39].

According to [39], although there are several challenges to exploit the full benefits of mmWave communications, the presented solutions and proposed techniques on mmWaves are very promising which makes mmWave as a key enabling technology for

5G and beyond networks. In the chapter to follow, a detailed explanation of the mmWave propagation and its unique characteristics along with solutions for the highly attenuated bands in mmWaves will be presented.

Chapter 3

Millimeter Wave Propagation

3.1 Introduction

The frequency band between 30 GHz and 300 GHz with the wavelengths from 10-1 mm generally termed as the extremely high frequency (EHF) band by ITU, is referred to as millimeter-wave as well. However, the super high frequency (SHF) spectrum ranging from (3-30) GHz or centimeter-waves, due to their similar propagation characteristics and specially in the context of 5G, has been referred to as millimeter waves as well. By this, the term millimeter wave is generally referred to bands (3-300) GHz [7].

The spectrum in the millimeter-wave band has been already utilized for some applications, such as, satellite communications, radars [42], and point to point communication, but not for wireless cellular networks until recently [9]. Probably, the unfavorable propagation characteristics of mmWaves, poor penetration through buildings and obstacles, high atmospheric absorption, and with high sensitivity to blockage had caused the mmWave spectrum to be largely remained unused.

Despite the high path loss and shadowing effects, mmWave frequencies remains highly attractive for future cellular networks [4]. Several studies recently reported multi-Gbps access communications using the mmWave [9], [35], [40]. The available large bandwidth at mmWaves, along with the processing techniques such as

beamforming (BF), highly directional antenna arrays, and of course massive MIMO makes the mmWave very suitable and optimal choice for dense networks and highly populated areas [38].

However, to utilize the full potential of mmWaves, the channel and characteristics of mmWave should be understood. In the next section we will overview the propagation characteristics of mmWave for 5G applications.

3.2 Millimeter Wave Spectrum

The current public cellular wireless communications use the microwave carrier frequency spectrum which is ranging from 700 MHz to 2.6 GHz with a total bandwidth of less than 780 MHz bandwidth [4]. However, there are much more frequency resources and bandwidth in the underdeveloped and underutilized high frequency spectrum between 30 GHz and 300 GHz, which is called millimeter wave, because of the wavelength of the spectrum ranging between 10 mm to 1 mm.

As shown in Figure 3.1 below, the potential available 252 GHz bandwidth is a huge resource for many wireless applications including the mobile broadband. Since Oxygen absorption and water vapor in the atmosphere causes high attenuation, [7] and limits the propagations in some parts of this spectrum, about a 100 GHz millimeter wave spectrum are available for mobile communications mainly at sub 100-GHz bands.

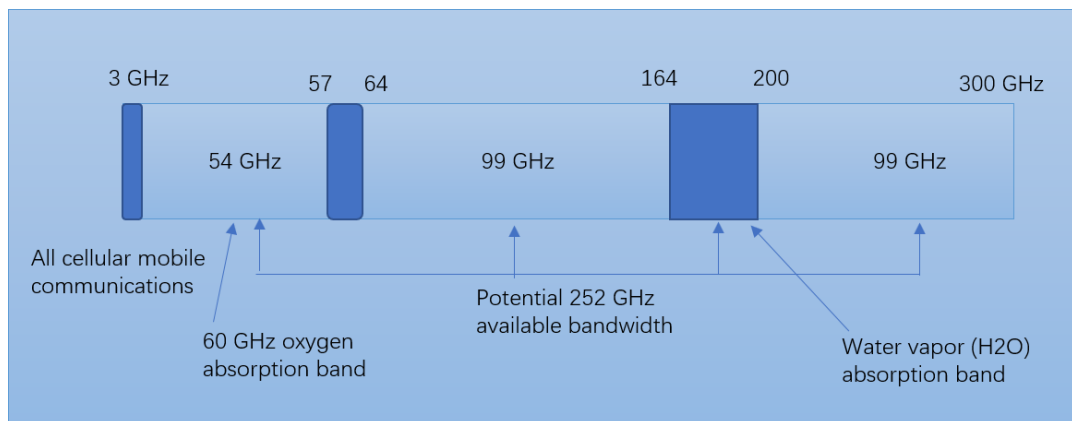


Figure 3.1 Millimeter wave spectrum, along with oxygen and water vapor absorption bands [7]

Based on the usage and wavelength of the sub-100 GHz bands, millimeter wave spectrum is divided and named into several bands.

Table 3.1 [41] shows these bands with related frequency range and wavelengths. In each of these bands, some applications have been considered by different countries. The Q band, generally ranging from 30 GHz to 50 GHz is mainly used for satellite communications, astronomy and terrestrial microwave communications. A part of the V band, from 50 GHz to 75 GHz is called 60 GHz and is used for unlicensed wireless communications [43]. Some parts of E band such as 71 GHz to 76 GHz, 81 GHz to 86 GHz and 92 GHz to 96 GHz has attracted attentions of standardization bodies for usage in fronthaul and backhaul networks specially in the United States [41]. The W band with small wavelength is suitable for satellite communications and deep space studies.

Table 3.1 Millimeter Wav frequency bands designation for sub-100 GHz [41]

Band designation	Frequency Range (GHz)	Wavelength (mm)
Q	30-50	10.00-6.00
U	40-60	7.50-5.00
V	50-75	6.00-4.00
E	60-90	5.00-3.33
W	75-110	4.00-2.73

Kei et al. [40], listed the mmWave spectrum frequencies selected for 5G and beyond by four different organizations including World Radio Conference-15 (WRC-15) in ITU-R, European Conference for Post and Telecommunication (CEPT) in EU, Federal Communication Commission (FCC) in the United States, and 5GMF [30] in Japan. The Table 3.2 shows that in addition to above 30 GHz bands, some parts of the 7 GHz bandwidth between 22 GHz and 29 GHz which is also called 24 GHz band and allocated for automotive radar will be used for 5G as well.

Table 3.2 Considered mmWave bands for 5G by different organizations [40]

WRC-15	CEPT	FCC	5GMF
24.25-27.25	24.25-27.25		
			24.75-31.0
		27.25-28.35	
			31.5-42.5
31.8-33.4	31.8-33.4	31.8-33.4	
37.0-40.5		37.0-38.6	
		38.6-40.0	
40.5-42.5	40.5-43.5	40.5-42.5	
42.5-43.5			
			45.3-47.0
45.5-47.0	45.5-48.9		
47.0-47.2			
47.2-50.2		47.2-50.2	47.0-50.2
50.4-52.6			50.4-52.6
		64.0-71.0	
66.0-76.0	66.0-71.0		66.0-76.0
	71.0-76.0	71.0-76.0	
81.0-86.0	81.0-86.0	81.0-86.0	81.0-86.0

3.3 Propagation Characteristics of MmWave at 5G Bands

As it was mentioned, the propagation characteristics of millimeter wave frequencies are different from the sub-3 GHz bands. Also, each frequency at the huge spectrum of millimeter wave has different propagation characteristics, therefore, studying the characteristics of the candidate bands for 5G helps toward better understanding and proper modeling of mmWave channels for various 5G deployments scenarios. In this section we will review the major propagation characteristics of millimeter wave, including free space propagation, atmospheric losses, rain attenuation, material penetration and reflection coefficients.

3.3.1 Atmospheric losses

Millimeter wave wireless communications suffer from a larger propagation loss that the gas molecules in the Earth's atmosphere cause, compared to microwave wireless systems at lower carrier frequencies. The atmospheric loss, which is called gaseous attenuation as well is caused by molecules absorbing some portion of propagating waves' energy and vibrating proportionally to the carrier frequency [9]. The severe attenuations in millimeter waves are caused by oxygen (O_2) gas and water vapor (H_2O) gas [8], [41], [44]. There are several other inter-related factors such as temperature, altitude, pressure and the most important one, operating carrier frequency that defines the intensity of gaseous absorption [9].

Figure 3.2 [39], a simplified and combined conclusion of oxygen and water vapor attenuation on the millimeter wave, shows that both dry air (oxygen) and water vapor have effects on the propagation of high frequency bands. Considering the sea level with the maximum air density as the worst case for atmospheric attenuation, the O_2

absorption peaks are observed at the 60 GHz with more than 10 dB/km and around 120 GHz at 1.4 dB/km loss respectively.

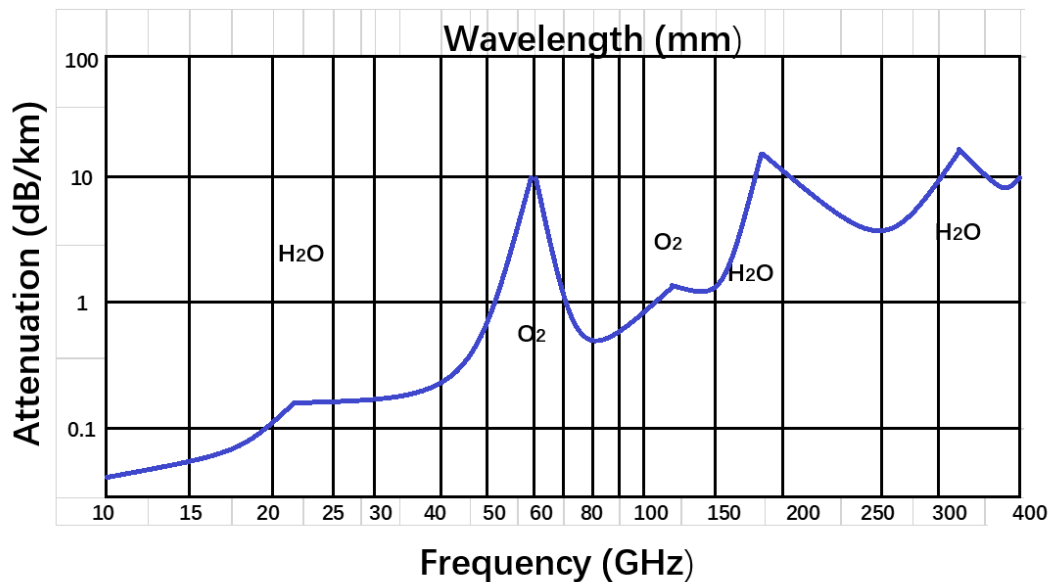


Figure 3.2 Specific attenuation of O_2 , H_2O and rain at sea level [39]

Also, it can be seen from the Figure 3.2 that the losses due to H_2O molecules are at 23 GHz and 183 GHz with associated losses of 0.18 dB/km and 28.35 dB/km respectively. It can be observed that the three large attenuations which are at 60 GHz, 183 GHz and around 323 GHz with the maximum attenuation of 38.6 dB/km at the latter, and two smaller peaks at 23 GHz and around 120 GHz, are generally called atmospheric attenuation resonant [8]. Since the O_2 and H_2O resonance bands do not match, it seems that the impact of atmospheric losses on millimeter wave is insignificant, especially on transmissions over short distances.

3.3.2 Rain attenuation

The precipitation attenuation and losses due to the rain are significant in millimeter waves. Raindrops are roughly at the same size that the radio wavelengths are at millimeter wave frequencies. Therefore, millimeter wave signals are easily blocked by raindrops, in which as a result, energy of the signal is scattered, and its strength is lost [8], [41]. Based on some reports, the rain attenuation depends on the rate of rainfall. It has been reported that for the heavier rain falls, the rain loss of the signal gets higher. The data from the experimental measurements at 70 GHz show that in a situation of light rain at 1 mm per hour the signal loss is around 0.9 dB/km and meanwhile, for a larger rain rate of 50 mm per hour an exponential increase to 18.4 dB/km is recorded.

In addition, the impact of rain is different on different frequency bands of millimeter waves. In the same rain rate, higher frequencies suffer larger rain losses. Compared to traditional wireless networks on microwave bands, rain attenuation at millimeter wave and designated sub-100 GHz bands for 5G are more problematic. However, with a shorter communication in the order of 200 m, the path loss due to rain attenuation is not significant. Thus, higher frequency millimeter waves are used in indoor scenarios and in the dense urban environments in a cell size not more than 200 meters.

3.3.3 Material Penetration

The millimeter wave frequencies are also vulnerable to penetration loss and compared to low frequency waves, the mmWave cannot propagate well through most of solid materials such as walls, doors, room furniture [9], [18]. Thus, millimeter wave signals are easily obstructed, especially in densely urban areas with lots of buildings and crowds of people. Several measurement campaigns such as [18], [19], [20], have

been carried out in different environments to study the penetrability and path loss of millimeter waves. The Table 3.3 shows the results of indoor and outdoor experiments by Zhao H. et al [18] in New York City in 2012. According the table, the mmWave suffer more from penetration loss in outdoor environments. For example, the tinted glass with 3.8 cm thickness experiences a 40.1 dB penetration loss in outdoor. Meanwhile, clear glass has the minimum penetration loss of 3.6 dB in the indoor condition.

Table 3.3 Penetration losses of different materials in dB/cm based on the measurements by [18]

Environment	Location	Material	Thickness (cm)	Penetration Loss (dB)
Outdoor	Othmer Residence Hall	Tinted Glass	3.8	40.1
	Warren Weaver Hall	Brick	185.4	28.3
Indoor	MetroTech Center	Clear Glass	<1.3	3.9
	Warren Weaver Hall	Tinted Glass	<1.3	24.5
		Clear Glass	<1.3	3.6
		Wall	38.1	6.8

3.4 Summary

In this chapter, we presented the propagation characteristics of millimeter wave communication. The mmWaves suffer from higher atmospheric attenuation and are sensitive to blockage. To fully utilize the mmWave potential, a well-understood characteristic of each band will be needed.

Chapter 4

Millimeter Wave Channel Modeling and System Design Consideration

4.1 Introduction

In the previous chapter, we discussed the fundamental characteristics of millimeter wave and explained how the mmWave characteristics are mainly different from traditional microwave bands. In this chapter, we discuss details of mmWave channel modelling, the available challenges toward it, and the considered large-scale and small-scale fading components. Also, in order to characterize the channel model which will be used in this work, urban micro and urban macro channel models will be considered. We will focus on the 5G Channel Model (5GCM) which will be used for simulations and discussion in this thesis.

4.2 The Millimeter Wave Channel Model

The extensive mmWave propagation measurements by various research teams, measurement campaigns, and trial deployments has resulted in the feasibility of mmWave for mobile communication, in which as a result, the utilization of mmWave

seems to be a reality for near future 5G cellular systems [4], [19], [20], [46], [47]. However, the design and deployment of an efficient 5G network in mmWaves, like any other wireless systems, needs channel models based on a thorough understanding of physical behavior and measurements to analyze signaling protocols and air interfaces [1], [41], [48].

The classification of channel models is done in to two categories of physical channel models and analysis-based channel models. The base for an analytical channel model is mathematical analysis, whilst the construction of a physical channel model is based on propagating signal characteristics between the transmitter and receiver antenna arrays [9]. In this work, we will consider the stochastic physical model which is based on extensive measurements, and the model is probabilistic for the description of the characteristics of spacial and temporal behavior of the multi path components (MPCs). The deterministic model generally has higher computational complexity. Another benefit of the stochastic channel models is its lower computational complexity with less time, which makes it suitable for simulation and system design [9].

4.3 Modelling Efforts in Millimeter Wave

The aims for utilization of mmWave for 5G different scenarios have accelerated channel modeling for carrier frequencies in the range of 2 GHz up to 100 GHz. Several projects and organizations have investigated and proposed channel models for various frequency bands such as 28 GHz, 38 GHz, 60 GHz, and 73 GHz, and for different deployment scenarios such as indoor, outdoor, backhaul, etc. [9], [48].

We will narrow down our focus only on the contributions on channel modeling for 5G technology. In Table 4.1 [9], [48], a number of major organizations that have contributed for channel modeling for 5G and for different environments such as LOS and NLOS and various frequency bands are listed.

Table 4.1 MmWave channel modeling by different organizations and efforts [9]

Technology	Frequency	year	Channel Model	Description
5G	28 GHz, 38 GHz, and 73 GHz	Since 2011	5GCM	A lot of research efforts on millimeter wave channel modeling mainly at 28 GHz, 38 GHz, and 73 GHz. Firstly, proposition on narrowband and then a number of wideband channels. [49]
5G	up to 100 GHz	2012	METIS	5G PPP millimeter wave channel model for mobile systems. The Model is according to WINNER II and WINNER + channel modeling [55].
5G	up to 100 GHz	2017	3GPP	The new 3GPP series 38.900 channel models which is an extension of 3GPP TR 36.873, commonly used for sub-6 GHz bands. The current model supports azimuthal and elevation characteristics of the channel. Different scenarios and sub-100 GHz bands are supported [31].
5G	6-100 GHz	15	mmMAGIC	An initiative of European Commission to investigate the employment of mmWaves for 5G. The mmMAGIC produced channel models based on intensive modelling and validation efforts benefiting a large amount of data from 22 channel measurement campaigns. [9], [50]

Table 4.1 shows the four major organizations' contribution to the mmWave channel modeling. We will suffice exploring these organizations to the descriptions in the table, unless for the 5GCM which will be used throughout this thesis and will be explained in detail. The efforts of 5G Channel Model is based on the extensive field measurements mainly at 28 GHz, 38 GHz, 60GHz, and 73GHz, by the NYU WIRELESS [26]. First a narrowband was proposed in [52] and then followed by wideband channel models of [20], [51]. Different scenarios including indoor, outdoor, device to device (D2D) and Vehicular-to-Vehicular (V2V) were considered in these channel models, with an emphasis on mobile access services [9].

According to [48], although many participants of these standardization bodies overlap, but the final models somewhat 'distinct' and recent work has found discrepancies between the proposed models and measured results. This shows that there are several modelling challenges, in which the developed models so far, cannot adequately reflect all features of mmWaves. In the next subsection, we will briefly overview some of these challenges.

4.4 Millimeter Wave Channel Modeling Challenges

Numerous channel models have been developed and exist in the literature, as the major ones were summarized in Table 4.1 in previous section. However, based on the mmWave use cases especially for 5G, huge bandwidth, and mmWave nature, these models cannot reflect all the characteristics of mmWaves. The main challenge is to develop a single channel model to be usable throughout the entire mmWave spectrum with only modifying the parameters in respect to carrier frequency, scenario case, or based on the used environment [9]. This was recognized by some organizations but claimed by [55] not to be achievable.

The main limitations of currently developed channel models are briefly highlighted in the areas of lack of measurements, huge bandwidth availability, dual mobility cases, directional antennas and massive array elements usage, which are among the challenging restrictions for the mmWave channel modeling [9], [48].

Although there have been extensive measurement campaigns at mmWaves, the wide range of mmWaves needs to be studied further. The previous models were developed for narrow bands of sub-6 GHz, in which the usage for the huge bandwidth of mmWave impose some limitations. In the device-to-device (D2D) communications that both nodes are moving, a higher Doppler spread is expected which affects the channel. The utilization of directional antennas along with massive antenna arrays or massive MIMO at mmWaves will mitigate the higher Doppler spread and high attenuations, and this needs to be considered in the channel modeling [9].

4.5 System Design Consideration

4.5.1 General Structure of mmWave Channel

In the mmWave channel, the aggregation of different multi path components with a short symbol interval forms the impulse response of the channel. A cluster can be defined as a number of MPCs which has similar tempo-spatial characteristics [9]. A model of aggregated channel matrix has been given in [9],

$$H(t) = \sum_{ncl}^{N_{cl}} \sum_p^{N_p} H_{ncl,p}(t) \quad (4.1)$$

where N_{cl} show the total number of aggregated clusters and N_p is the number of the rays in the cluster, meanwhile $H_{ncl,p}(t)$ is a single multipath of p -th ray in the n_{cl} -th cluster at time t . In the literature, the path loss is commonly considered in the LOS and NLOS scenarios. We will briefly explain each scenario in the follows.

4.5.2 LOS Probability Model

In the literature on mmWave, it is common to describe the path loss for LOS and NLOS conditions separately. Therefore, a model is needed to predict whether a user equipment (UE) is within a clear LOS of a base station (BS) or is obstructed to be in an NLOS region [48]. The LOS probability is frequency-independent and is modeled as a function of distance between transmitter and receiver, which can be affected by environment layout.

4.5.2.1 UMi LOS Probability

As it was mentioned in the section 2.2 of chapter 2, the UMi scenario is defined for high user density areas with an inter-site distance (ISDs) of up to 200 m and BS height below rooftops. Different organizations have developed the UMi LOS probability models as shown in the Table 4.2 [48] below. We will suffice explaining for the 5GCM which will be used throughout this thesis and will be explained in detail.

Table 4.2 LOS probability models of 5GCM in the UMi and UMa scenarios [48]

UMi	<p>d1/d2 model: $P_{LOS}(d_{2D}) = \min(d1/d_{2D}, 1) (1 - \exp(-d_{2D}=d2)) + \exp(-d_{2D}=d2)$</p> <p>NYU (squared) model: $P_{LOS}(d_{2D}) = (\min(d1/d_{2D}, 1) (1 - \exp(-d_{2D}/d2)) + \exp(-d_{2D}=d2))^2$</p>	<p>d1/d2 model: $d1 = 20 \text{ m}, d2 = 39 \text{ m}$</p> <p>NYU (squared) model: $d1 = 22 \text{ m}, d2 = 100 \text{ m}$</p>
UMa	<p>d1/d2 model: $P_{LOS} = (\min(d1=d_{2D}, 1) (1 - \exp(-d_{2D}/d2)) + \exp(-d_{2D}/d2)) (1 + C(d_{2D}, h_{UE}))$</p> <p>NYU (squared) model: $P_{LOS} = ((\min(d1/d_{2D}, 1) (1 - \exp(-d_{2D}/d2)) + \exp(-d_{2D}/d2)) (1 + C(d_{2D}, h_{UE})))^2$</p>	<p>d1/d2 model: $d1 = 20 \text{ m}, d2 = 66 \text{ m}$</p> <p>NYU (squared) model: $d1 = 20 \text{ m}, d2 = 160 \text{ m}$</p>

Table 4.2 shows the contribution of the 5GCM [49] for UMi and UMa scenarios which has introduced two LOS probability models in each scenario. The first one is similar to the 3GPP TR 38.901 outdoor model described in the literature, with slight difference in d_1 and d_2 values. The second one is NYU squared model [53], which adds a square on the last term. This model was developed based on intensive measurements in New York City [48].

4.5.2.2 UMa LOS Probability

In the Urban Macrocell (UMa) scenario, the UE height is in the ground level at 1.5 m and BSs are typically mounted above rooftop at heights 25-30 m, and with an ISD up to 500 m [32]. The UMa LOS probabilities are given in the previous Table 4.2 [48], as well, which are identical to UMi LOS probability, with only differences in the d_1 and d_2 values.

4.5.3 Large-Scale Path Loss Models

Out of the three basic types of large-scale path loss models which are used for predicting the signal strength over distances, we use the close-in (CI) free space reference distance model with 1 m reference distance, throughout this work. The CI path loss is frequency dependent and use a close-in reference distance according to Friis' law and given by [48], [54]:

$$PL^{CI}(f_c, d_{3D}) [\text{dB}] = \text{FSPL}(f_c, 1\text{m}) + 10n \log_{10}(d_{3D}) + \chi_{\sigma}^{CI} \quad (4.2)$$

where $\chi_{\sigma}^{\text{CI}}$ is the shadow fading (SF) as a zero mean Gaussian random variable with a standard deviation in dB, n is the path loss exponent (PLE), $d_{3D} > 1\text{m}$, FSLP) (f_C , 1m) is the free space path loss at frequency f_C in GHz at 1 m and the FSPL is calculated as:

$$\text{FSPL}(f_C, 1\text{m}) [\text{dB}] = 20\log_{10}(4\pi f_C \times 10^9/c) = 32.4 + 20\log_{10}(f_C) [\text{dB}] \quad (4.3)$$

where c is the speed of light in a vacuum, 3×10^8 m/s. The CI links path loss of different frequencies to the free space path loss at 1 m according to the Friis' law and researches report that it has shown more accuracy and less complexity [50], comparing with others. The path loss models are generally created omnidirectional with the assumption of unity gain antennas [48].

4.5.3.1 UMi Large-Scale Path LOS

The UMi scenario is commonly considered as street canyon or open square situations, as it can be seen in the Table 4.3 [48]. The 5GCM [49] has chosen the CI for modeling the UMi LOS path loss. In the CI path loss model, only the Path Loss Exponent (PLE), a single parameter, is determined to minimize the model error of mean loss over distance through optimization. However, in the Floating Intercept (FI) also known as ABG model, three parameters namely α , β and γ need to be optimized to minimize the model error [48].

Table 4.3 Omnidirectional Path loss models in the UMi scenario [48]

	PL [dB], f_c is in GHz and d_{3D} is in meters	Shadow fading std [dB]	Applicability range and Parameters
5GCM [12]			
5GCM UMi-Street Canyon LOS	CI model with 1 m reference distance: $PL = 32.4 + 21 \log_{10}(d_{3D}) + 20 \log_{10}(f_c)$	$\sigma_{SF} = 3.76$	$6 < f_c < 100$ GHz
5GCM UMi-Street Canyon NLOS	CI model with 1 m reference distance: $PL = 32.4 + 31.7 \log_{10}(d_{3D}) + 20 \log_{10}(f_c)$ ABG model: $PL = 35.3 \log_{10}(d_{3D}) + 22.4 + 21.3 \log_{10}(f_c)$	$\sigma_{SF} = 8.09$ $\sigma_{SF} = 7.82$	$6 < f_c < 100$ GHz
5GCM UMi-Open Square LOS	CI model with 1 m reference distance: $PL = 32.4 + 18.5 \log_{10}(d_{3D}) + 20 \log_{10}(f_c)$	$\sigma_{SF} = 4.2$	$6 < f_c < 100$ GHz
5GCM UMi-Open Square NLOS	CI model with 1 m reference distance: $PL = 32.4 + 28.9 \log_{10}(d_{3D}) + 20 \log_{10}(f_c)$ ABG model: $PL = 41.4 \log_{10}(d_{3D}) + 3.66 + 24.3 \log_{10}(f_c)$	$\sigma_{SF} = 7.1$ $\sigma_{SF} = 7.0$	$6 < f_c < 100$ GHz
3GPP TR 38.901 V14.0.0 [101]			
3GPP UMi-Street Canyon LOS	$PL_{UMi-LOS} = \begin{cases} PL_1, & 10 \text{ m} \leq d_{2D} \leq d'_{BP} \\ PL_2, & d'_{BP} \leq d_{2D} \leq 5 \text{ km} \end{cases}$ $PL_1 = 32.4 + 21 \log_{10}(d_{3D}) + 20 \log_{10}(f_c)$ $PL_2 = 32.4 + 40 \log_{10}(d_{3D}) + 20 \log_{10}(f_c) - 9.5 \log_{10}((d'_{BP})^2 + (h_{BS} - h_{UE})^2)$ where d'_{BP} is specified in Eq. (8)	$\sigma_{SF} = 4.0$	$0.5 < f_c < 100$ GHz $1.5 \text{ m} \leq h_{UE} \leq 22.5 \text{ m}$ $h_{BS} = 10 \text{ m}$
3GPP UMi-Street Canyon NLOS	$PL = \max(PL_{UMi-LOS}(d_{3D}), PL_{UMi-NLOS}(d_{3D}))$ $PL_{UMi-NLOS} = 35.3 \log_{10}(d_{3D}) + 22.4 + 21.3 \log_{10}(f_c) - 0.3(h_{UE} - 1.5)$ Option: CI model with 1 m reference distance $PL = 32.4 + 20 \log_{10}(f_c) + 31.9 \log_{10}(d_{3D})$	$\sigma_{SF} = 7.82$ $\sigma_{SF} = 8.2$	$0.5 < f_c < 100$ GHz $10 \text{ m} < d_{2D} < 5000 \text{ m}$ $1.5 \text{ m} \leq h_{UE} \leq 22.5 \text{ m}$ $h_{BS} = 10 \text{ m}$
METIS [102]			
METIS UMi-Street Canyon LOS	$PL_{UMi-LOS} = \begin{cases} PL_1, & 10 \text{ m} < d_{3D} \leq d_{BP} \\ PL_2, & d_{BP} < d_{3D} \leq 500 \text{ m} \end{cases}$ $PL_1 = 22 \log_{10}(d_{3D}) + 28.0 + 20 \log_{10}(f_c) + PL_0$ $PL_2 = 40 \log_{10}(d_{3D}) + 7.8 - 18 \log_{10}(h_{BS} h_{UE}) + 2 \log_{10}(f_c) + PL_1(d_{BP})$ d_{BP} and PL_0 are specified in Eq. (9) and (10)	$\sigma_{SF} = 3.1$	$0.8 \leq f_c \leq 60$ GHz
METIS UMi-Street Canyon NLOS	$PL = \max(PL_{UMi-LOS}(d_{3D}), PL_{UMi-NLOS}(d_{3D}))$ $PL_{UMi-NLOS} = 36.7 \log_{10}(d_{3D}) + 23.15 + 26 \log_{10}(f_c) - 0.3(h_{UE})$	$\sigma_{SF} = 4.0$	$0.45 \leq f_c \leq 6$ GHz $10 \text{ m} < d_{2D} < 2000 \text{ m}$ $h_{BS} = 10 \text{ m}$ $1.5 \text{ m} \leq h_{UE} \leq 22.5 \text{ m}$
mmMAGIC [92]			
mmMAGIC UMi-Street Canyon LOS	$PL = 19.2 \log_{10}(d_{3D}) + 32.9 + 20.8 \log_{10}(f_c)$	$\sigma_{SF} = 2.0$	$6 < f_c < 100$ GHz
mmMAGIC UMi-Street Canyon NLOS	$PL = 45.0 \log_{10}(d_{3D}) + 31.0 + 20.0 \log_{10}(f_c)$	$\sigma_{SF} = 7.82$	$6 < f_c < 100$ GHz
Note : PL is path loss. d_{3D} is the 3D T-R Euclidean distance. All distances or heights are in meters and frequency related values are in GHz, unless it is stated otherwise.			

4.5.3.2 UMa Large-Scale Path LOS

The 5GCM [49] has introduced three UMa path loss models, CI, CI with a frequency-weighted (CIF) and ABG. The ABG and CIF are considered for the NLOS scenario while CI is used for the LOS condition. The path loss models of 5GCM and other organizations are explained in the Table 4.4 [48] below.

Table 4.4 Omnidirectional Path loss models in the UMa scenario

	PL [dB], f_c is in GHz, d is in meters	Shadow fading std [dB]	Applicability range and Parameters
5GCM [12]			
5GCM UMa LOS	CI model with 1 m reference distance: $PL = 32.4 + 20 \log_{10}(d_{3D}) + 20 \log_{10}(f_c)$	$\sigma_{SF} = 4.1$	$6 < f_c < 100$ GHz
5GCM UMa NLOS	CI model with 1 m reference distance: $PL = 32.4 + 30 \log_{10}(d_{3D}) + 20 \log_{10}(f_c)$ ABG model: $PL = 34 \log_{10}(d_{3D}) + 19.2 + 23 \log_{10}(f_c)$	$\sigma_{SF} = 6.8$ $\sigma_{SF} = 6.5$	$6 < f_c < 100$ GHz
3GPP TR 38.901 V14.0.0 [101]			
3GPP TR 38.901 UMa LOS	$PL_{UMa-LOS} = \begin{cases} PL_1, & 10 \text{ m} \leq d_{2D} \leq d'_{BP} \\ PL_2, & d'_{BP} \leq d_{2D} \leq 5 \text{ km} \end{cases}$ $PL_1 = 28.0 + 22 \log_{10}(d_{3D}) + 20 \log_{10}(f_c)$ $PL_2 = 28.0 + 40 \log_{10}(d_{3D}) + 20 \log_{10}(f_c) - 9 \log_{10}((d'_{BP})^2 + (h_{BS} - h_{UE})^2)$ where $d'_{BP} = 4h'_{BS}h'_{UE}f_c \times 10^9/c$	$\sigma_{SF} = 4.0$	$0.5 < f_c < 100$ GHz $1.5 \text{ m} \leq h_{UE} \leq 22.5 \text{ m}$ $h_{BS} = 25 \text{ m}$
3GPP TR 38.901 UMa NLOS	$PL = \max(PL_{UMa-LOS}(d_{3D}), PL_{UMa-NLOS}(d_{3D}))$ $PL_{UMa-NLOS} = 13.54 + 39.08 \log_{10}(d_{3D}) + 20 \log_{10}(f_c) - 0.6(h_{UE} - 1.5)$ Option: CI model with 1 m reference distance $PL = 32.4 + 20 \log_{10}(f_c) + 30 \log_{10}(d_{3D})$	$\sigma_{SF} = 6.0$ $\sigma_{SF} = 7.8$	$0.5 < f_c < 100$ GHz $10 \text{ m} < d_{2D} < 5000 \text{ m}$ $1.5 \text{ m} \leq h_{UE} \leq 22.5 \text{ m}$ $h_{BS} = 25 \text{ m}$
METIS [102]			
METIS UMa LOS	$PL_{UMa-LOS} = \begin{cases} PL_1, & 10 \text{ m} \leq d_{2D} \leq d'_{BP} \\ PL_2, & d'_{BP} \leq d_{2D} \leq 5 \text{ km} \end{cases}$ $PL_1 = 28 + 22 \log_{10}(d_{3D}) + 20 \log_{10}(f_c)$ $PL_2 = 28 + 40 \log_{10}(d_{3D}) + 20 \log_{10}(f_c) - 9 \log_{10}((d'_{BP})^2 + (h_{BS} - h_{UE})^2)$ where $d'_{BP} = 4(h_{BS} - 1)(h_{UE} - 1)f_c \times 10^9/c$	$\sigma_{SF} = 4.0$	$0.45 < f_c < 6$ GHz $10 \text{ m} < d_{2D} < 5000 \text{ m}$ $1.5 \text{ m} \leq h_{UE} \leq 22.5 \text{ m}$ $h_{BS} = 25 \text{ m}$
METIS UMa NLOS	$PL = \max(PL_{UMa-LOS}(d_{3D}), PL_{UMa-NLOS}(d_{3D}))$ $PL_{UMa-NLOS} = 161.94 - 7.1 \log_{10}(w) + 7.5 \log_{10}(h) - \left(24.37 - 3.7 \left(\frac{h}{h_{BS}}\right)^2\right) \log_{10}(h_{BS}) + (43.42 - 3.1 \log_{10}(h_{BS}))(\log_{10}(d_{3D}) - 3) + 20 \log_{10}(f_c) - 0.6(h_{UE})$	$\sigma_{SF} = 6.0$	$0.45 < f_c < 6$ GHz $10 \text{ m} < d_{2D} < 5000 \text{ m}$ $1.5 \text{ m} \leq h_{UE} \leq 22.5 \text{ m}$ $h_{BS} = 25 \text{ m}$ $w = 20 \text{ m}$ $h = 20 \text{ m}$

4.6 Considered Model for Urban Dense Environments

Among the existing channel models developed by different groups, 5GCM [49], and 3GPP channel models are mostly referenced to in this thesis. In this research, the NYUSIM simulator [56] is used for all simulations as it has been shown in [53] that it has more accuracy than 3GPP. The NYUSIM simulator has been developed by NYU WIRELESS at the New York University, and is based on the channel modeling of 5GCM [49], benefiting from extensive mmWave field measurements in various cities in the United States and in the Republic of Korea. For the dense urban environment of this research case, we will consider the UMi and UMa scenarios with different frequency bands, and with the 5GCM developed channel models.

Chapter 5

Performance Evaluation and Discussion

In this chapter we evaluate and compare the performance of mmWave large-scale fading such as path loss, shadowing factor and delay spread through simulations on the three considered frequencies of 28 GHz, 73 GHz and 4 GHz for the dense urban environments.

5.1 Simulation Setup

Our simulation set up consisting of channel parameters and antenna properties for an outdoor millimeter wave propagation is as follows. We have simulated 28 GHz and 73 GHz frequencies for UMi scenario with an 800 MHz bandwidth over MIMO channel of 16X4 ULA antenna arrays. Also, for the UMa scenario, 4 GHz with a 200 MHz bandwidth, based on the requirements of 3GPP 5G NR, is simulated with an 8X2 ULA arrays. Both scenarios are simulated in the NYUSIM, simulator [56]. The NYUSIM simulator uses the Close-in approach for path loss calculation as was discussed in chapter 4. The simulator contains all the parameters affecting the radiation of mmWave including the large-scale parameters of Line-of-Sight (LOS), Non- Line-of Sight (NLOS) and path loss, and, small-scale parameters such as foliage attenuation. The propagation frequency range of the simulator is from 0.5 GHz to 100 GHz and has considered different scenarios of Urban Micro (UMi), Urban Macro (UMa) and Rural Macro (RMa).

The channel parameters and antenna design properties at NYUSIM simulator are set as follows. For the propagation properties, the UMi and UMa scenarios are considered with both Line-of-Sight (LOS) and Non-Line-of-Sight (NLOS) and the TX-RX separation distance is ranging from 10 to 500 m. The atmospheric effects including barometric pressure, humidity, temperature and rate rain are specified as 1015 mbar, 50%, 10 °C and 5 mm/hr, a typical weather condition in January in Tokyo, respectively. The foliage attenuation is 0.4 dB/m and the distance between the foliage is set to 10 m in any randomly selected location. The channel parameters and antenna properties are set as shown in Table 5.1.

Table 5.1 Channel parameters and Antenna Properties for UMi and UMa scenarios

Channel Parameters	Specification	
	UMi Scenario	UMa Scenario
Carrier Frequency	28 GHz, 73 GHz	4 GHz
Bandwidth	800 MHz	200 MHz
Height of BS	25 m	Not considered
Temperature	10 °C	
TX-RX Separation	10-500 m	
Number of RX locations	500	
Foliage attenuation	0.4 dB/m x 10 m	
Distance within foliage	10 m	
TX Power	30 dBm	
TX Array Type, N _t	ULA, 16	ULA, 8
RX Array Type, N _r	ULA, 4	ULA, 2
TX Antenna Spacing	0.5 λ	
RX Antenna Spacing	0.5 λ	
Modulation	OFDM	

5.2 Simulation Results

As it was mentioned in the previous section, the simulations have been conducted on three frequencies which are among the list of frequencies to be used in 5G access systems, namely, 28 GHz and 73 GHz for the urban microcell (UMi) scenario of radius not more than 200 meters, and 4 GHz for the urban microcell (UMa) of up to 500 m for dense urban environments. Since path loss and shadowing are the two important variations in the propagation and determining the received signal power, we show the simulation results of the channel extracting the values for these variations. Generally, path loss and shadowing are mainly caused by transmission distance and obstruction in the signal path, therefore we evaluate these variations for the LOS and NLOS cases under the directional and omnidirectional conditions for different distances for the considered frequencies. Also, directional and omnidirectional power delay profiles (PDPs) for each considered frequency are compared in LOS or NLOS cases, and among the simulated frequencies.

5.2.1 Dense urban microcell (UMi) scenario

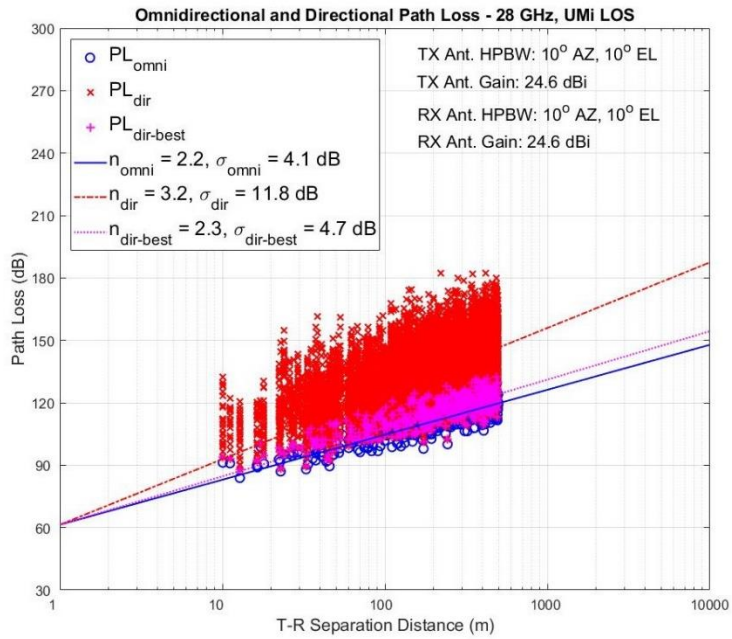
As we explained in section 2.3, the main characteristics of the dense urban environment is outdoor and outdoor-to-indoor coverage with high traffic loads. Considering the high penetration loss at mmWave and as authors in [12] also proposed splitting the outdoor and indoor 5G access, our focus on this work is on the outdoor UMi scenario which seems to be the main deployment of 5G for dense urban areas with few dozen meters of Inter-Site-Distance (ISDs). In this section, we will investigate the performance of 28 and 73 GHz bands with the range of TX-RX distances at 200 m and 100 m respectively, for both LOS and NLOS cases. The performance of each case will be considered for both omnidirectional and directional conditions. The PDPs of LOS

cases are compared for the directional and omnidirectional conditions for each utilized frequency at a randomly TX-RX distance as well.

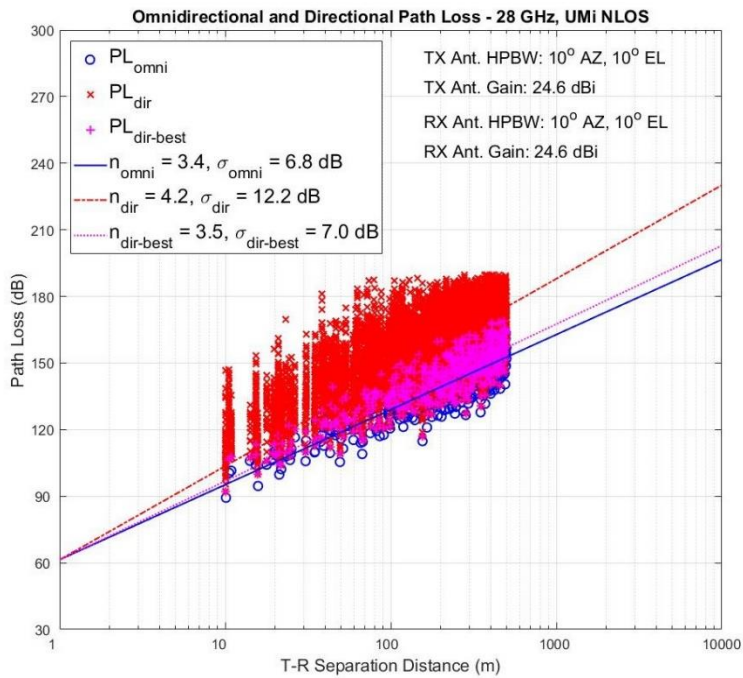
5.2.1.1 28 GHz performance

In our simulation the first carrier frequency is the frequency band of 28 GHz. The 28 GHz frequency band enjoys very interest and popularity for the future 5G mmWave access, although it was excluded from the WRC-15 nominated bands for IMT-2020 deployments [12]. Also, according to 5GMF [30], most of the mmWave field measurements for 5G in Japan are conducted in 28 GHz and 4 GHz, which both probably have the support of Japanese government in the WRC-19 for 5G bands.

The simulations result of the directional and omnidirectional path loss, the aggregated path loss exponent (PLE) and directional best PLE for the LOS and NLOS cases is shown in the Figure 5.1. The figure depicts the performance at 500 randomly selected RXs by NYUSIM simulator [56] ranging from 10 m to 500 m, as the lower and upper bounds from the TX respectively, and under the channel parameters described in previous section.



(a)

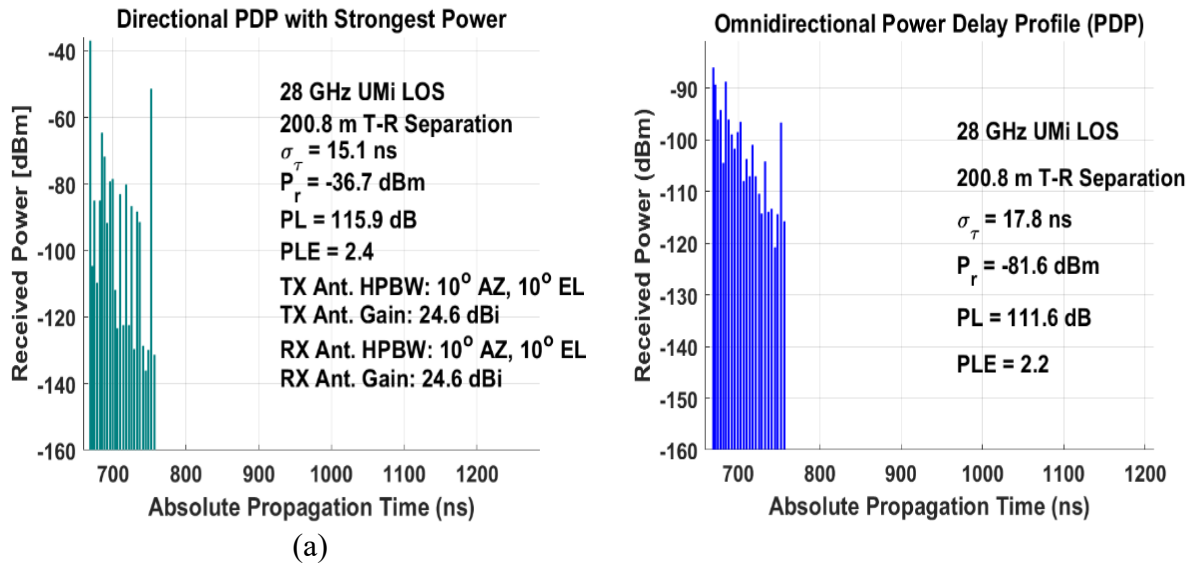


(b)

Figure 5.1. Omnidirectional and directional path loss values generated with 500 simulation runs for the 28 GHz UMi, (a) LOS and (b) NLOS scenarios. n denotes the path loss exponent (PLE), σ is the shadow fading standard deviation, "omni" represents omnidirectional, "dir" denotes directional, "dir-best" means the direction with the strongest received power, "Ant." denotes antenna, "AZ" and "EL" stand for azimuth and elevation, respectively.

The Figure 5.1 shows that the path loss increases linearly as distance increases and it is higher for directional propagations in both cases and is even highest under the NLOS conditions. Figure 5.1 (a) shows that directional PLE at 3.2 with a shadowing factor (SF) $\sigma_{\text{dir}}=11.8$ dB is higher than the omnidirectional PLE of 2.2 and $\sigma_{\text{omni}}=4.1$ dB, as in the literature for the LOS. However, the directional best PLE, or strongest possible link created in directional path, is very close to omnidirectional PLE. Moreover, as seen in Figure 5.1 (b), the path loss increases faster for the NLOS scenario than LOS, with regards to increase in distance due to obstruction on the signal path. For the directional path in NLOS case, the PLE increases to 4.2 and with a shadowing factor of 12.2, dB, yet a with a directional best value of only 0.1 and 0.2 dB, PLE and SF respectively, higher than in the omnidirectional propagation. The results suggest that higher directional PLE for both NLOS and LOS cases in 28 GHz is probably because antenna arrays are often not optically aligned on boresight. This problem can be addressed by using steerable beam antennas as investigated in [19]. The results also suggest that omnidirectional propagation path loss at 28 GHz is not drastically higher than those in the current microwave systems within the UMi scenario.

Figure 5.2 shows the directional power delay profile (PDP) with strongest power and the omnidirectional PDP for the 28 GHz at a randomly selected RX location at 200.8 m in the UMi LOS case. The path loss and PLE of both directional and omnidirectional conditions show small difference, as it can also be seen for the RMS delay spread (σ_{τ}) with a short time difference. However, the received signal power for omnidirectional is more than two times weaker than in directional. The simulation results are comparable to the field measurements in [6], [20] and [46] as well. The results suggest that directional propagation in LOS case is not much greater than omnidirectional for the smaller cells of up to 200 m at 28 GHz.



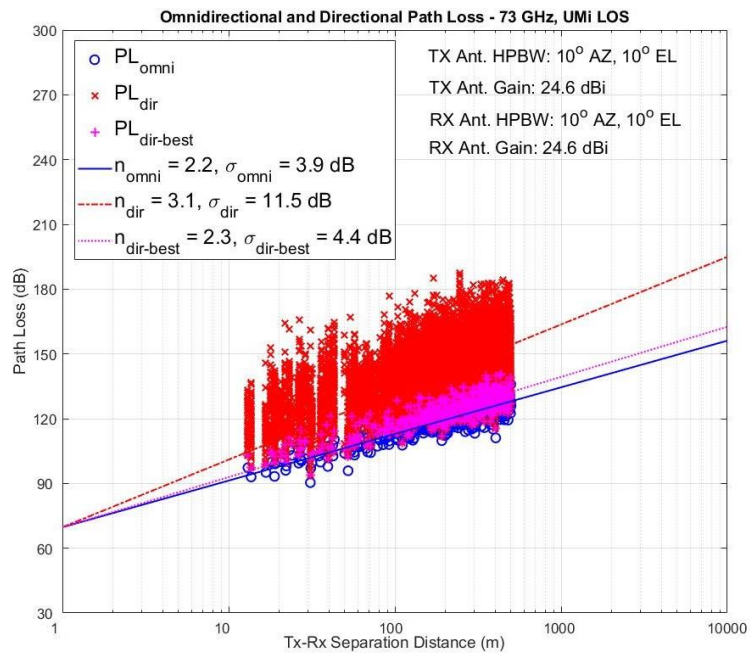
(b)

Figure 5.2 Omnidirectional PDP and Directional Power Delay Profiles with strongest power at 28 GHz at 200.8 m TX-RX separation in UMi LOS case. "Ant." denotes antenna.

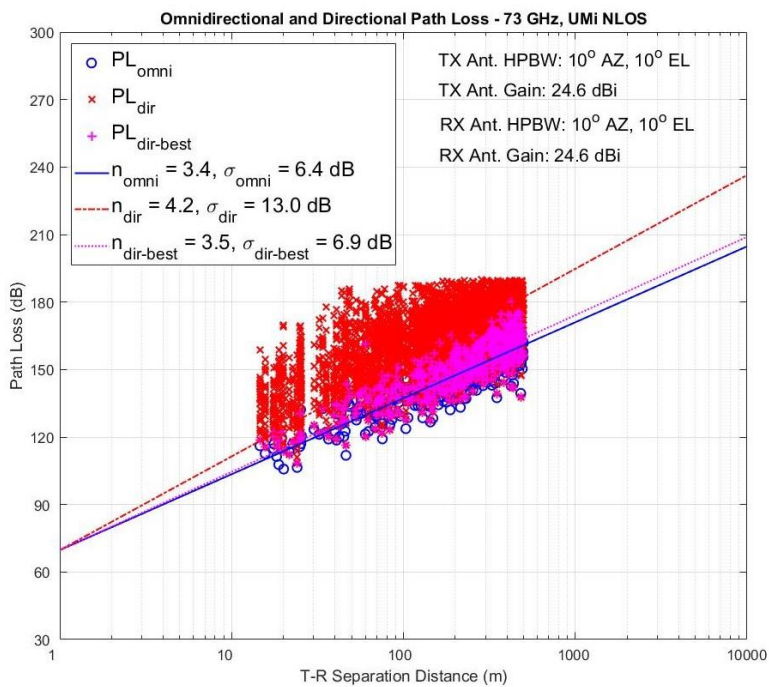
5.2.1.2 73 GHz performance

The 73 GHz band is another popular frequency that has attracted interests from academia for research and industry for commercial applications. Researchers achieved multi-Gigabit per second wireless links at 73 GHz and it has been used for 5G trial by some companies as well. It is still a popular frequency band for 5G deployments in urban areas.

The simulation results of 73 GHz band of the directional and omnidirectional path loss, the PLE and directional best PLE for the LOS and NLOS cases is shown in the Figure 5.3.



(a)



(b)

Figure 5.3 Omnidirectional and directional path loss values generated with 500 simulation runs for the 73 GHz UMi, (a) LOS and (b) NLOS scenarios.

Similar to the 28 GHz, Figure 5.3 shows that the path loss increases linearly as distance increases and it is higher for directional propagations in both cases.

Figure 5.3 (a) shows that the PLE and SF of 73 GHz is smaller than 28 GHz under the same channel condition. On the other hand, Figure 5.3 (b), shows that for the NLOS case in the 73 GHz, multipath components (MPCs) are not detectable as a threshold of 168 dB path loss floor as was set for measurement campaign in [19]. The results suggest that 73 GHz is applicable for both LOS and NLOS in the ISDs less than 100 m for the dense urban areas cellular networks as shown in [51].

Figure 5.4 shows the PDPs for directional and omnidirectional propagations at 73 GHz at 101.9 m. Similar to 28 GHz, there are small differences in PLE and PL. However, it can be seen that ratio of the omnidirectional to directional delay spread, σ_τ in this UMi LOS case is in the order of 4 times which is higher than to field measurements [46]. The results suggest that omnidirectional delay spread for LOS at 73 GHz is greater meanwhile, it receives much higher number of multipath component than directional propagation.

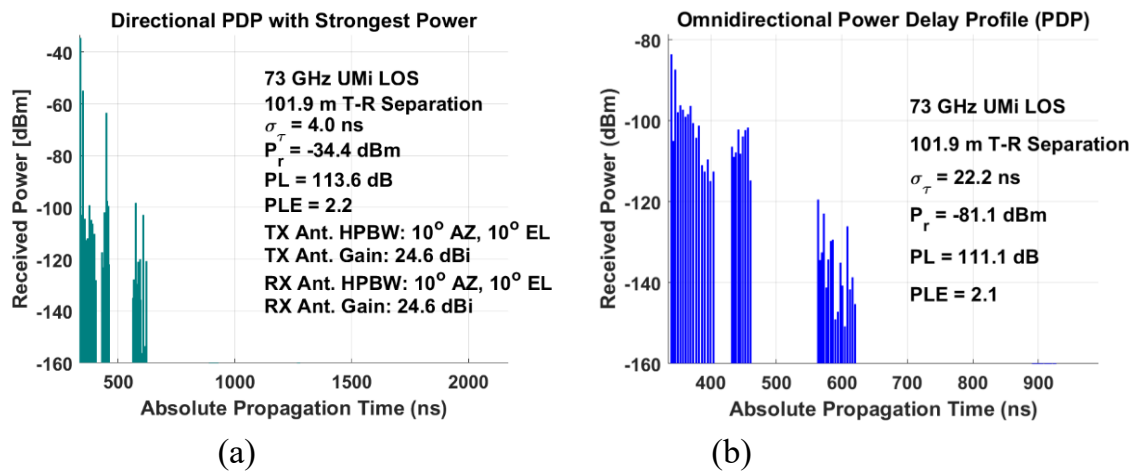


Figure 5.4 Omnidirectional PDP and Directional Power Delay Profiles with strongest power at 73 GHz at 101.9 m UMi LOS case. "Ant." denotes antenna.

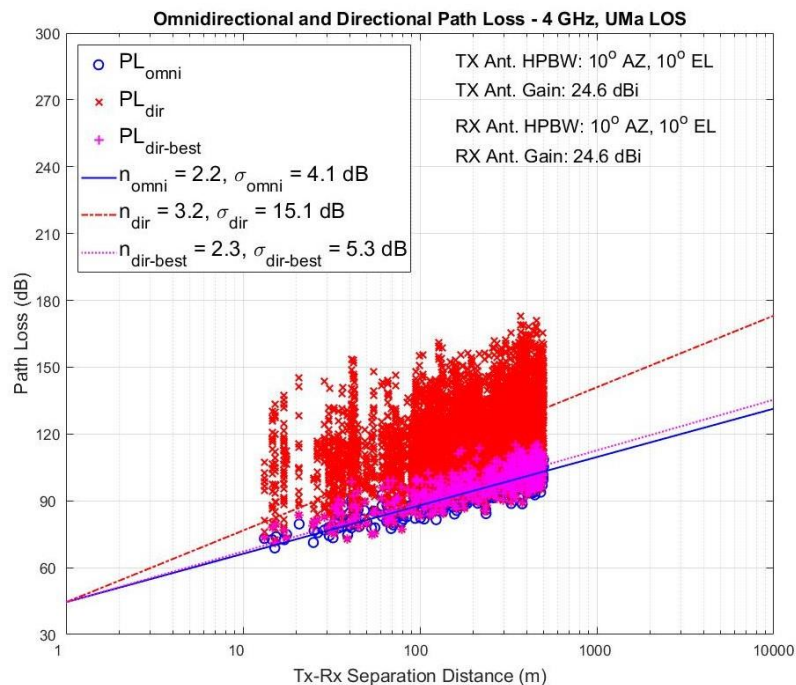
5.2.2 Dense urban macro (UMa) scenario

The urban macro scenario for a millimeter wave deployment was illustrated in section 2.3 based on 3GPP [31] definition. The ISD for this scenario is up to 200 m since our frequency is 4 GHz, we will consider a cell radius of 500 m for this case.

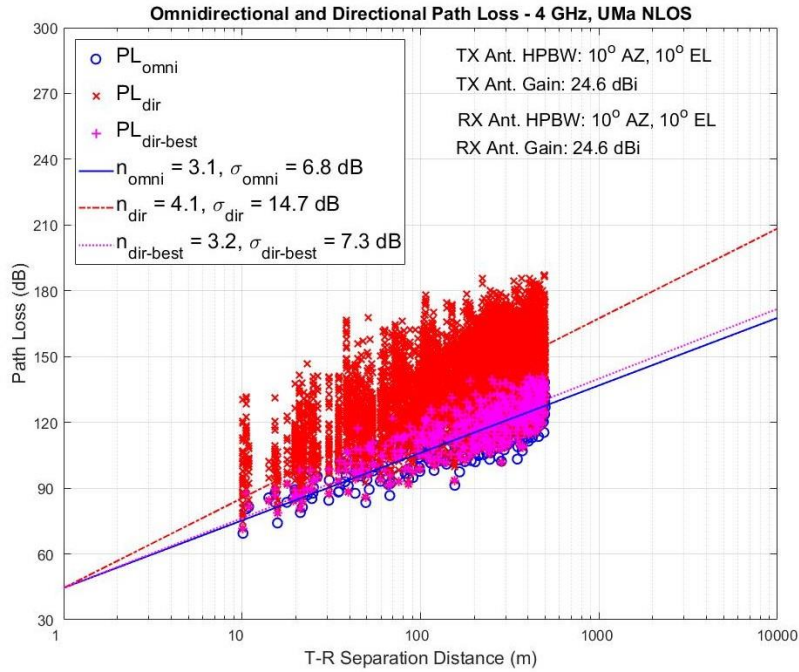
5.2.1.3 4 GHz Performance

The 4 GHz has attracted many attentions recently to be among the bands which will be allocated for 5G in WRC-19. Some countries such as japan has already started field measurements and tests on this frequency [3].

Similar to the 28 GHz and 73 Ghz, we will examine the path loss, PLE and best PLE for 4 GHz band as well. However, for the PDPs the NLOS case has been considered for 4 GHz. Figure 5.5 shows the simulated path loss for different conditions.



(a)



(b)

Figure 5.2.1 Omnidirectional and directional path loss values generated with 500 simulation runs for the 4 GHz UMa, (a) LOS and (b) NLOS scenarios.

Figure 5.5 Omnidirectional and directional path loss values generated with 500 simulation runs for the 4 GHz UMa, (a) LOS and (b) NLOS scenarios.

Since 4 GHz is a sub-6 GHz band, based on the 3GPP [31] recommendation, a wide bandwidth of up to 200 MHz can be used in this band for application in 5G. Figure 5.5 shows that the PLE of both LOS and NLOS of 4 GHz is similar to the 28 GHz and 73 GHz. However, Figure 5.5 (a) shows that the SF at $\sigma_{dir}=15.1$ dB is larger than both previous frequencies. Similarly, shadow factor for NLOS is greater than other studied frequencies. Next, we will observe the PDPs performance for this frequency band in Figure 5.6.

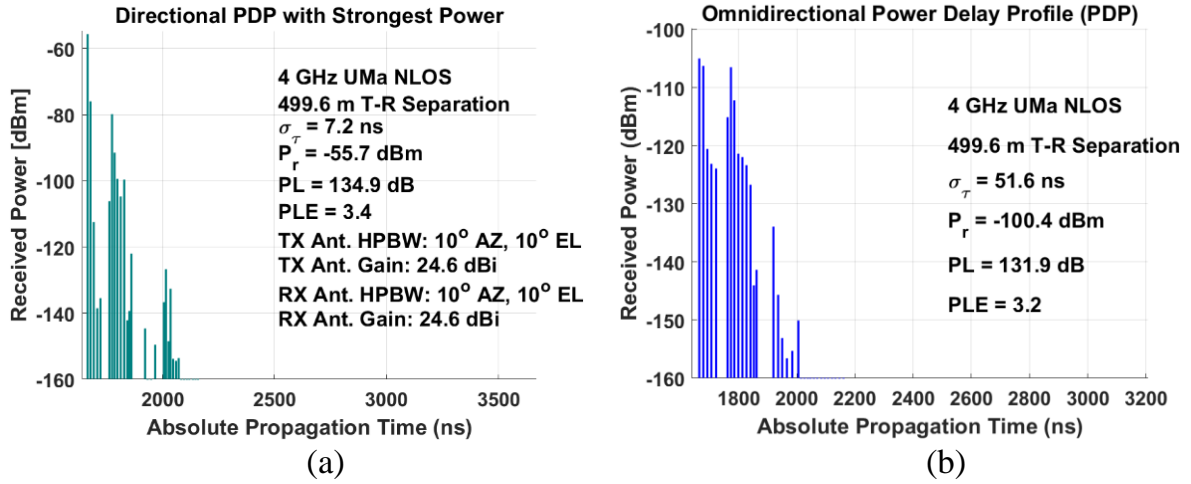


Figure 5.6 Omnidirectional PDP and Directional Power Delay Profiles with strongest power at 4 GHz at 499.6 m UMa NLOS case. "Ant." denotes antenna.

Figure 5.6 shows the PDPs for directional and omnidirectional propagations at 4 GHz at 499.6 m TX-RX separation. Similar to 28 GHz and 73 GHz, the PLE and PL are close in values in each case. However, it can be seen that ratio of the omnidirectional to directional delay spread, σ_τ in this UMa NLOS case is in the order of 7 times which is aligned with the field measurements [46]. The results suggest that a number of multiple components are detectable for NLOS case at 4 GHz in the range of 500 m, with a comparable path loss to other mmWave frequencies.

The results of this study show that the considered mmWave frequency bands have the capability to be used in the 5G mobile network, by overcoming some propagation challenges, for all scenarios. Simulations have shown that propagation in microcell in LOS and NLOS cases has path loss within the compensable range for propagation. The results also suggest that using microcells of less than 100 m for 73 GHz, 200 m for 28 GHz and up to 500 m for 4 GHz will suited for 5G access transmission. However, it should be taken into account that based on report in [46], the outage probability for 28 GHz within 200 m is about 20 %, but it increases dramatically to 57 % beyond 200 m.

Chapter 6

Conclusion and Future Work

6.1 Conclusion

Millimeter Wave communication is a key enabling technological for the realization of the Internet of Things in the 5G and beyond networks. In this thesis, we studied the propagation characteristics of mmWave in a dense urban environment for a heterogenous 5G network. The results in this study show that mmWave has the capabilities to be used in the 5G cellular outdoor networks by overcoming some propagation challenges for the massive connectivity in the dense urban areas.

We reviewed the propagation characteristics of millimeter wave and highlighted the differences that mmWaves show in terms of higher rain and atmosphere attenuation and more sensitivity to blockage, compared to traditional wireless communications. The efforts for mmWave channel modeling was discussed and some developed channel models were introduced. We also described the details of the considered channel model for urban dense environments.

We finally presented the performance evaluation of the 28 GHz, 73 GHz and 4 GHz mmWave bands in a dense UMi and UMa environment. The results have shown that propagation in this environment in LOS and NLOS cases has path loss within the compensable range for propagation. However, the path loss in the NLOS case for

directional propagation is higher compared to omnidirectional path loss and increases rapidly with increase in the distance.

In conclusion, large-scale characteristics of the studied mmWave bands have shown good potentials for usage in the urban dense area. High gain directional antenna arrays with massive MIMO are considered to overcome the severe path loss challenges in some specific circumstances.

6.2 Future Work

As an extension, our future work will investigate other mmWave propagation scenarios such as Outdoor-to-Indoor (O2I) and penetration into buildings which poses other challenges towards deployment of mmWave in the 5G and beyond wireless networks. Also, we will focus on the directional transmissions at mmWave frequencies employing massive antenna arrays, to study and propose efficient beamforming techniques mitigating directional propagation loss. This leads to consider time-efficient beam training techniques for estimation of channel state information at mmWaves with narrower beams and with high directionality as well. In this regard, our future work focus will be on consideration of innovative algorithms for channel estimation in designing hybrid beamforming as a promising architecture for future mmWave mobile communications.

Research Achievements

1. Ahmad S. Seraj and Takuro Sato, “Propagation Challenges for 5G MillimeterWave-enabled Communication Systems: The UMi Scenario”, The 37th JSST Annual International Conference on Simulation Technology, Hokkaido, Japan, Sep. 2018

References

- [1] T. S. Rappaport et al., *Millimeter Wave Wireless Communications*. Pearson/Prentice Hall, 2015.

- [2] Cisco Visual Networking Index: Forecast and Trends, 2017–2022, Cisco, Nev. 2018. [Online]. Available: <https://www.cisco.com/c/en/us/solutions/collateral/service-provider/visual-networking-index-vni/white-paper-c11-741490.pdf>

- [3] Cisco Visual Networking Index: Forecast and Trends, 2012–2017, Cisco, May 2013. [Online]. Available: http://www.davidellis.ca/wp-content/uploads/2012/08/cisco-vni_c11-481360.pdf

- [4] T. S. Rappaport et al “Millimeter Wave Mobile Communications for 5G Cellular: It will work!” *IEEE Access*, vol. 1, pp. 335-349, May 2013.

- [5] H. Zhang, S. Venkateswaran, and U. Madhow, “Channel modeling and MIMO capacity for outdoor millimeter wave links”, in *Proc. IEEE Wireless Commun. Netw. Conf. (WCNC)*, Sydney, NSW, Australia, Apr. 2010, pp. 1–6.

- [6] T. S. Rappaport et al., “Broadband millimeter-wave propagation measurements and models using adaptive-beam antennas for outdoor urban cellular communications,” *IEEE Trans. Antennas Propag.*, vol. 61, no. 4, pp. 1850–1859, Apr. 2013.

- [7] Z. Pi and F. Khan, “An Introduction to Millimeter-Wave Mobile Broadband Systems”, *IEEE Communications Mag.*, vol. 49, no. 6, pp. 101–107, Jun. 2011.

- [8] Adhikari, P. “Understanding millimeter wave wireless communication”, Loea Corp., White paper, 2008.

- [9] Ibrahim A. Hemadeh et al. “Millimeter-Wave Communications: Physical Channel

Models, Design Considerations, Antenna Constructions, and Link-Budget”, IEEE Comm. Surv. & Tutorials., Vol. 20, No.2, May 2018.

- [10] A. Gupta and R. K. JHA, “A Survey of 5G Network: Architecture and Emerging Technologies” IEEE Access, Vol. 3, pp. 1206-1232, July 2015.
- [11] Cheng Xiang Wang et al. “Cellular Architecture and key technologies for 5G wireless communication”, IEEE Comm. Magazine, Vol., pp. 121-130, Feb. 2014.
- [12] W. Xiang, K. Zheng, X. Shen, 5G Mobile Communications, Switzerland: Springer International Publishing, 2017.
- [13] P. Agyapong, M. Iwamura, D. Staehle, W. Kiess, and A. Benjebbour, “Design considerations for a 5G network architecture,” IEEE Comm. Mag., Vol. 52, No. 11, pp. 65–75, Nov. 2014.
- [14] J. Zhang et al., “5G Millimeter-Wave Antenna Array: Design and Challenges” IEEE Wireless Communications, pp. 106-112, April 2017.
- [15] Diego Dupleich, et al., “A Hybrid Polarimetric Wide-Band Beam-former Architecture for 5G mm-Wave Communications. WSA 2016 Munich, Germany, pp 32-39.
- [16] J. G. Andrews, et al., "What Will 5G Be?", IEEE Journal on selected areas in communications, Vol. 32, No. 6, pp. 1065-1077, June 2014.
- [17] RP-160689, “Study on Scenarios and Requirements for Next Generation Access Technologies”, 3GPP TR 38.913 V0.3.0, March 2016.
- [18] H. Zhao et al., “28 GHz millimeter wave cellular communication measurements for reflection and penetration loss in and around buildings in New York city,” in Proc. IEEE Int. Conf. Comm. (ICC), Budapest, Hungary, pp. 5163–5167, Jun. 2013.

- [19] Y. Azar, et al., “28 GHz Propagation Measurements for Outdoor Cellular Communications Using Steerable Beam Antennas in New York City”, in IEEE ICC Wireless Communications Symposium, pp. 5143-5147, 2013.
- [20] T. S. Rappaport et al., “Wideband Millimeter-Wave Propagation Measurements and Channel Models for Future Wireless Communication System Design” IEEE Trans. on Comm., Vol. 63, No. 9, pp. 3029-3056, Sep. 2015.
- [21] Andrea Goldsmith, Wireless Communications, Cambridge University Press 2005.
- [22] T. S. Rappaport, Wireless Communication, 2nd ed., Prentice Hall, 2010.
- [23] Pekka P. “A Brief Overview of 5G Research Activities”, in 1st International Conference on 5G for Ubiquitous Connectivity (5GU), pp. 17-22, Nov. 2014.
- [24] Horizon 2020 - The EU Framework Programme for Research and Innovation. [Online]. Available: <http://ec.europa.eu/programmes/horizon2020/>
- [25] The 5G Infrastructure Public Private Partnership. [Online]. Available: <http://5g-ppp.eu/>
- [26] New York University WIRELESS research center (NYU WIRELESS) [Online]. Available: <https://wireless.engineering.nyu.edu/>
- [27] 5G Americas [Online]. Available: <http://www.5gamericas.org/en/>
- [28] IMT-2020 (5G) Promotion Group in China [Online]. Available: <http://www.imt2020.org.cn/en>
- [29] 5G forum [Online]. Available: <https://www.5gforum.org/english>
- [30] The Fifth Generation Mobile Communication Promotion Forum (5GMF). [Online]. Available: <https://5gmf.jp/en/>
- [31] 3rd Generation Project Partnership [Online]. Available: <http://www.3gpp.org/>

- [32] Recommendation ITU-R M.2083-0, “IMT Vision–Framework and overall objectives of the future development of IMT for 2020 and beyond”, Sep. 2015. [Online]. Available: <https://www.itu.int/rec/R-REC-M.2083-0-201509-I/en>.
- [33] S. Sun et al., “Investigation of prediction accuracy, sensitivity, and parameter stability of large-scale propagation path loss models for 5G wireless communications,” *IEEE Transactions on Vehicular Technology*, vol. 65, no. 5, pp. 2843–2860, May 2016.
- [34] E. G. Larsson, et al. “Massive MIMO for Next Generation Wireless Systems”, *IEEE Vehicular Technology Magazine*, Oct. 2015.
- [35] T. E. Bogale, and L. B. Le, “Massive MIMO and Millimeter Wave for 5G Wireless HetNet: Potentials and Challenges”, *IEEE Communications Magazine*, pp. 186-195, Feb. 2014.
- [36] S. Sun, T. S. Rappaport, and M. Shafi, “Hybrid beamforming for 5G millimeter-wave multi-cell networks,” in *Proceedings of the IEEE Conference on Computer Communications Workshops (INFOCOM WKSHPS)*, Honolulu, HI, USA, Apr. 2018.
- [37] Ibrahim A. et al. “toward 5G Network Slicing over Multiple-Domains” in *IEICE Trans. Commu.*, Vol. E100-B, No.11, Nov. 2017.
- [38] Ge X., et al. “5G Ultra-Dense Cellular Networks”, in *IEEE Wireless Communications*, pp. 72-79, Feb. 2016.
- [39] Niu, Y., Li, Y., Jin, D., Su, L. and Vasilakos, A. “A survey of millimeter wave communications (mmWave) for 5G: opportunities and challenges.”, *Wireless Networks*, 21(8), pp.2657-2676. 2015.
- [40] K. SAKAGUCHI et al., “Where, When, and How mmWave is Used in 5G and Beyond” in *IEICE TRANS. ELECTRON.*, VOL.E100–C, NO.10 Oct. 2017.

- [41] M. Marcus and B. Pattan, "Millimeter wave propagation; spectrum management implications," *IEEE Microw. Mag.*, Vol. 6, No. 2, pp. 54–62, Jun. 2005.
- [42] E. Damosso, L. Stola, and G. Brussaard, "Characterization of the 50-70 GHz band for space communications," *ESAJ.*, Vol. 7, No. 1, pp. 25-43, 1983.
- [43] R. C. Daniels, J. N. Murdock, T. S. Rappaport, and R. W. Heath, "60 GHz wireless: Up close and personal", *IEEE Microw. Mag.*, vol. 11, no. 7, pp. 44–50, Dec. 2010.
- [44] Frenzel, L. "Millimeter Waves Will Expand the Wireless Future. [online] *Electronic Design*", 2017. Available at: <http://www.electronicdesign.com/communications/millimeter-waves-will-expand-wireless-future>.
- [45] S. Deng, M. K. Samimi, and T. S. Rappaport, "28 GHz and 73 GHz millimeter-wave indoor propagation measurements and path loss models," in *IEEE International Conference on Communications Workshops (ICCW)*, pp. 1244–1250, Jun. 2015.
- [46] C. U. Bas, et al., "28 GHz microcell measurement campaign for residential environment" *IEEE GLOBECOM*, Dec. 2017.
- [47] Ahmad S. Seraj and Takuro Sato, "Propagation Challenges for 5G MillimeterWave-enabled Communication Systems: The UMi Scenario", *The 37th JSST Annual International Conference on Simulation Technology*, Hokkaido, Japan, Sep. 2018.
- [48] T. S. Rappaport et al., "Overview of Millimeter Wave Communications for Fifth-Generation (5G) Wireless Networks-with a focus on Propagation Models" *IEEE Trans. on Antennas and Propagation*, Special Issue on 5G, Nov. 2017.
- [49] 5GCM, "5G Channel Model for bands up to 100 GHz," *Tech. Rep.*, Oct. 2016. [Online]. Available: <http://www.5gworkshops.com/5GCM.html>
- [50] S. Sun et al., "Propagation Path Loss Models for 5G Urban Micro- and

Macro-Cellular Scenarios,” in 2016 IEEE 83rd Vehicular Technology Conference (VTC 2016-Spring), pp. 1–6, May 2016.

- [51] T. S. Rappaport and S. Deng, “73 GHz wideband millimeter-wave foliage and ground reflection measurements and models,” in 2015 IEEE International Conference on Communication Workshop (ICCW), pp. 1238–1243, June 2015.
- [52] M. Akdeniz et al., “Millimeter wave channel modeling and cellular capacity evaluation,” IEEE J. Sel. Areas Comm., vol. 32, no. 6, pp. 1164–1179, Jun. 2014.
- [53] T. S. Rappaport et al., “Investigation and Comparison of 3GPP and NYUSIM Channel Models for 5G Wireless Communications”, IEEE VTC, Toronto, Canada, Sep. 2017
- [54] H. T. Friss, “A note on a simple transmission formula,” proc. IRE, vol. 34, No.5, pp. 254-256, May 1946.
- [55] METIS2020, “METIS Channel Model,” Tech. Rep. METIS2020, Deliverable D1.4 v3, July 2015. [Online]. Available: [https://www.metis2020.com/wp-content/uploads/deliverables/METIS D1.4 v3.0.pdf](https://www.metis2020.com/wp-content/uploads/deliverables/METIS_D1.4_v3.0.pdf)
- [56] S. Sun, G. R. MacCartney, and T. S. Rappaport, “A novel millimeter-wave channel simulator and applications for 5G wireless communications”, in 2017 IEEE International Conference on Communications (ICC), May 2017, pp. 1–7. [Online]. Available: <https://arxiv.org/pdf/1703.08232.pdf>.